ASTRONOMY & ASTROPHYSICS
SUPPLEMENT SERIES

Astron. Astrophys. Suppl. Ser. **117,** 1-11 (1996)

Penetrating the "zone of avoidance".⋆ II. Optically detected galaxies in the region $180° \leq l \lesssim 240°$

R. Seeberger, W. Saurer and R. Weinberger

Institut für Astronomie der Leopold-Franzens-Universität Innsbruck, Technikerstraße 25, A-6020 Innsbruck, Austria

Received January 27; accepted September 14, 1995

Abstract. — We have carried out a systematic search for galaxies in the galactic plane in a ten degree wide strip ($-5° \leq b \leq +5°$). In an area of 300 square degrees between $\ell = 180°$ and $\ell = 210°$, 755 galaxies have been detected on Palomar red-sensitive prints. The smallest galaxies show diameters of 0.1 mm corresponding to $6\farcs7$. We extended our survey to $\delta = -27°$ i.e. $\ell \approx 247°$ to check our catalogue for completeness by comparing it with the Saitō et al. (1990, 1991) catalogues of galaxies and present 334 new galaxy candidates at $\ell \geq 210°$. An asymmetry with respect to the galactic equator is obvious. By assuming the 60 μ and 100 μ sky flux density to be a rough measure of the total interstellar galactic extinction, and comparing them with the surface densities of the galaxies, we detected one possible galaxy cluster candidate at $(\ell, b) \approx (181\fdg5, +3\fdg5)$, a concentration of galaxies at $(\ell, b) \approx (195°, +4\fdg5)$, and confirmed three other galaxy concentrations. Finally, we argue that the red-sensitive surveys (ESO R; POSS II-R, POSS II-IR) are the best suitable material for galaxy searches in the zone of avoidance.

Key words: catalogues and dictionaries — galaxies: general — interstellar medium: extinction — Universe (the): structure of

1. Introduction

Searches for extragalactic sources behind the Milky Way are of interest for several research fields: i) Large-scale structures in the Universe that should be pursued also across the "zone of avoidance" (ZOA), ii) the origin of the peculiar velocity of the Local Group as a whole and other streaming motions, iii) detection of additional massive members of or very near to the Local Group in order to better understand the extent and dynamics of the latter, and iv) to better model the dust distribution in our Galaxy. For these purposes a number of searches and studies have been started in recent years by various groups of astronomers. We began an extensive optical survey in late 1989 along the entire northern Galactic Plane on prints of the Palomar Observatory Sky Survey I (POSS I) and will present our results in this series of articles.

In a previous paper (Weinberger et al. 1995, hereafter Paper I) we have compiled all published optically identified extragalactic objects within $|b| \leq 5°$, altogether 2304 entries. Mainly because of two Schmidt-plate based surveys (Saitō et al. 1990, 1991) and optical confirmation of IRAS-colour-selected galaxy candidates (Yamada et al. 1993; Takata et al. 1994) most galaxies known near the galactic plane are in the southern hemisphere. The reasons for that are the deepness, sensitivity, and fine grain emulsion of ESO/SERC Schmidt-plates.

Until completion of the Palomar Observatory Sky Survey II (POSS II) (1999 or 2000) the best available homogeneous plate material of the northern sky remains the POSS I. Weinberger (1980) has shown that the POSS I red prints are well suited for a galaxy search even very close to the galactic plane ($|b| \leq 2°$). These prints have very recently been used for a search for galaxies in the region $90° \leq \ell \leq 110°$, $-10° \leq b \leq +10°$ that led to the detection of 1346 galaxy candidates (Seeberger 1994).

In this paper we present a catalogue of galaxies behind the Milky Way within $|b| \leq 5°, 180° \leq \ell \lesssim 240°$. A part of this region was also included in the survey of Saitō et al. (1990, hereafter S90), who have chosen $\ell \approx 210^{\rm o}$ as their northern limit. In the overlap zone with the S90 survey ($\ell \geq 210°$) we present additional galaxy candidates.

2. The search procedure

In principle there are several procedures to search for galaxies behind the galactic plane:
Selection of galaxies from the IRAS-PSC: Far-infrared emission can be used to select candidate galaxies (e.g.

Send offprint requests to: W. Saurer

⋆Tables 2 and 3 are only available in electronic form: see the Editorial in A&A 1994, Vol. 103, No. 1

Table 1. The Palomar prints used for this survey

No.	δ(1950)	α(1950)	seeing ($''$)	No.	δ(1950)	α(1950)	seeing ($''$)
411	+30°	06h 04m	3(3)	1346	00°	06h 48m	1-2(1-2)
1459	+30°	05h 38m	2(2)	1483	00°	06h 24m	2(2)
23	+24°	06h 30m	2(2)	1495	−06°	07h 36m	2-3(2-3)
1278	+24°	06h 04m	3(3)	1488	−06°	07h 12m	2-3(2-3)
416	+24°	05h 38m	2(2)	653	−06°	06h 48m	2(2)
454	+24°	05h 12m	2(1-2)	943	−06°	06h 24m	3-4(3)
1470	+18°	06h 24m	1-2(1-2)	1521	−12°	07h 36m	4(3)
1494	+18°	06h 00m	2-3(2)	1619	−12°	07h 12m	3(3)
427	+18°	05h 36m	2(2)	436	−12°	06h 48m	3(2)
428	+12°	06h 48m	2-3(1-2)	1010	−18°	08h 00m	2(2)
445	+12°	06h 24m	1(1)	683	−18°	07h 36m	1-2(1-2)
1502	+12°	06h 00m	1(1)	647	−18°	07h 12m	1-2(1-2)
929	+06°	06h 48m	2(3)	1343	−18°	06h 48m	2(2)
923	+06°	06h 24m	2(1-2)	921	−24°	08h 14m	2(3)
229	+06°	06h 00m	3(3)	420	−24°	07h 48m	2-3(2-3)
1491	00°	07h 12m	2(2)	656	−24°	07h 22m	3(3)

Helou 1986; Lu et al. 1990; Takata et al. 1994). This method samples irregular galaxies and spirals. However, ellipticals which harbour almost no dust will be missed.

Systematical blind searches in the 21 cm line: Blind searches reveal a detection rate of only 0.5% (Kerr & Henning 1987; Henning 1992). This method is very time consuming when applied to the whole galactic plane and to a large velocity range. A survey of the whole northern galactic plane ($v \leq 4000$ km/s) was recently started (Burton & Hartmann 1994).

Automatical scanning of Schmidt-plates: This method is applied at higher galactic latitudes (e.g. Maddox et al. 1990). However, in the ZOA search algorithms for galaxies fail because of the large number of disturbing stars.

Visual inspection of Schmidt-plates: This is the only method to get a more or less complete sample concerning Hubble type, but highly obscured galaxies will be missed.

For our survey we used paper prints of the Palomar Observatory Sky Survey. Using a binocular at 16-fold magnification and illumination from below (diffuse objects are more easily recognizable this way) we surveyed 32 POSS I-E (red) prints for faint galaxies. The POSS field numbers together with the central coordinates and the seeing in red and - in parentheses - blue, are listed in Table 1.

We included all overlap zones on the prints in our survey. Because of the multiple inspection of these overlap zones a higher completeness could be expected within these areas. On the other hand, the quality of the POSS prints decreases at the outer parts.

The smallest diameters of the galaxies searched are 0.1 mm corresponding to $6\farcs7$. In some cases it was not straightforward to decide whether the detected objects are galaxies, other types of galactic objects or plate flaws. For this reason we checked if the objects are also visible on POSS I-O prints (blue). However, due to galactic extinction almost all galaxies are fainter and/or smaller on POSS I-O. Many of the galaxies are visible in the Infrared Survey (Hoessel et al. 1979) in spite of its lower limiting magnitude and lower quality. Those objects that have defied a secure classification are marked with a colon in our catalogue. Follow-up observations in the 21 cm line at Effelsberg (Seeberger et al. 1994) have, however, shown that approximately one third of such objects have been detected in HI, the same percentage as for a sample of galaxies without a colon.

3. Galaxy distribution between 180° and 210° longitude

3.1. *The catalogue*

Table 2 lists 755 galaxies, arranged with increasing galactic longitude. The galaxy designations follow the IAU-recommendation for the nomenclature of new objects: ZOAG G$\ell\ell\ell.\ell\ell\pm bb.bb$. ZOAG means Zone Of Avoidance Galaxy. G stands for galactic coordinates. $\ell\ell\ell.\ell\ell$ and $\pm bb.bb$ are galactic longitude and latitude, respectively.

In Col. 1 the name of the galaxy is listed. For reason of brevity the prefix ZOAG G is omitted. Galaxies with identical galactic coordinates are followed by a suffix "a" or "b" (see Paper I).

Columns 2 and 3 give the equatorial coordinates for equinox 1950.0 (Bessel), Cols. 4 and 5 for equinox 2000.0 (Julian).

Columns 6 to 8 enable to identify the galaxies on the POSS I. In Col. 6 the POSS I field number is listed. Columns 7 and 8 give the cartesian coordinates (in mm) of the galaxies with the origin of the system at the south-east corner of the fields. Both cartesian and equatorial coordinates were measured using a high resolution digitizer and a software developed at Innsbruck. A set of 7 to 10 standard stars taken from the SAO-catalogue was used to compute these coordinates. More than 100 galaxies that are visible on more than one Palomar print were measured twice in order to calculate the accuracy. The overall

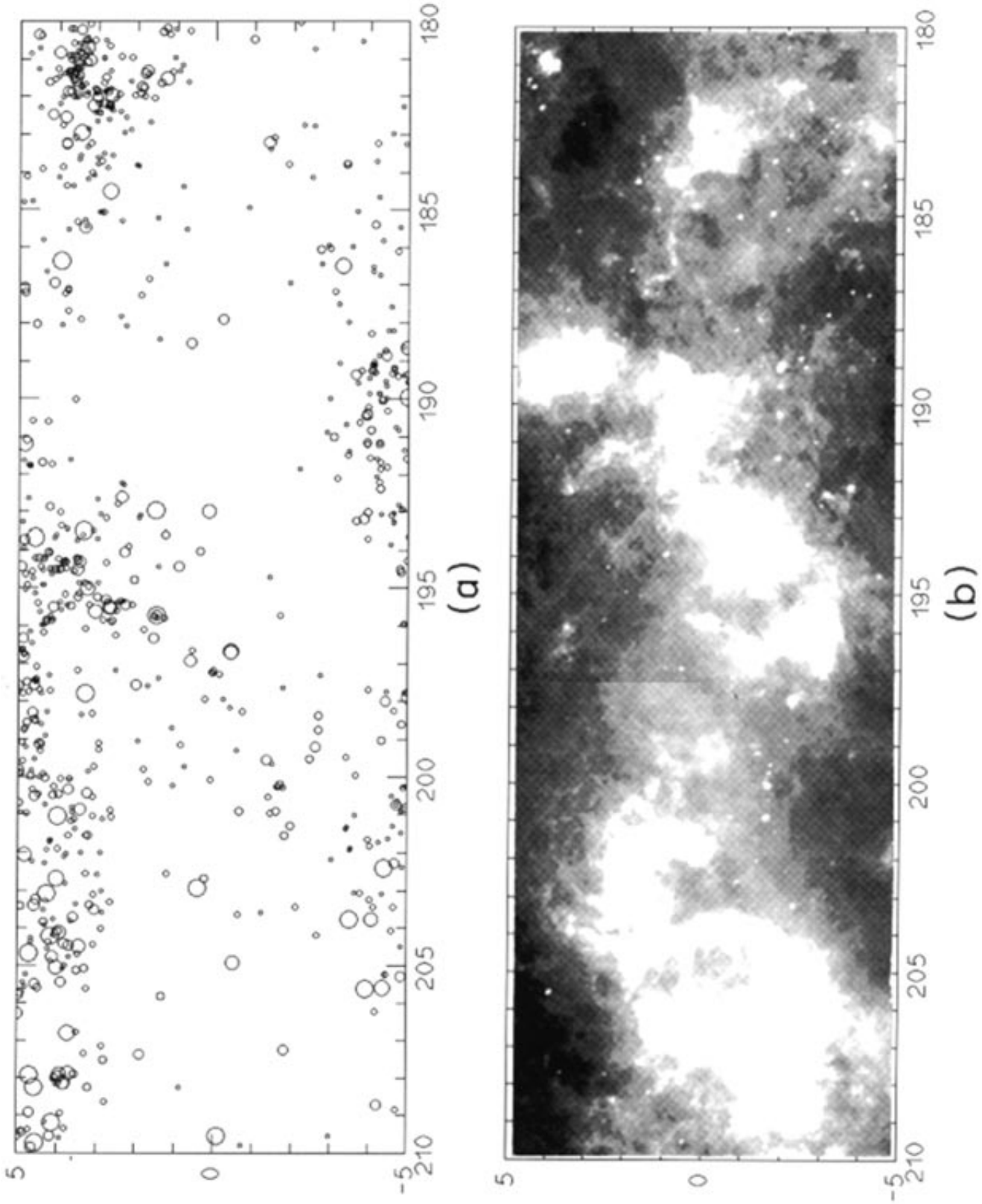

Fig. 1. a) Distribution of the new galaxies in galactic coordinates; the diameters of the open circles are proportional to the apparent size of the galaxies on POSS I-E; **b)** the 60 μ flux density taken from the IRAS Sky Survey Atlas. Black (white) areas correspond to low (high) flux densities. **(To be seen in landscape)**

accuracy turned out to be $\pm 6''$, whereas the resolution of the digitizer is about $1''$.

Columns 9 and 11 give the maximum diameters (in arcmin) measured from POSS-E (red sensitive) and POSS-O (blue sensitive), respectively. In many cases a core surrounded by a diffuse nebulosity can clearly be discerned. In Cols. 10 and 12 the core diameters measured on the red and blue prints are listed. Although a morphological classification of reddened galaxies is rather uncertain (Cameron 1990) we decided to classify in Col. 13 (t=type) spirals as S and probable spirals as S?.

In Col. 14 both usual galaxy names (in accordance with Paper I) and IRAS-PSC designations are listed. We used an optical positional uncertainty in α and δ of $\pm 0'.1$ and checked whether our optical error bars fall within the IRAS uncertainty ellipse or not. The 4 cases were we found two galaxies located inside one IRAS error ellipse are marked by asterisks to the IRAS name.

3.2. *The distribution*

When investigating the large scale structure of galaxies, mainly the effects of the patchily distributed dust, which will produce artificial over- and/or underdensities of galaxies should be taken into account. Figures 1a, b shows all detected galaxies in the region $180° \leq \ell \leq 210°$ together with a grey scale map of the $60\,\mu$ flux densities taken from the IRAS Sky Survey Atlas (Wheelock et al. 1991) using the software provided by SkyView (World Wide Web).

In Fig. 1a the diameters of the open circles are proportional to the apparent size of the galaxies on POSS I-E. Galaxies with diameters of $0'.10$ and $0'.15$ were plotted using the smallest symbol. The next symbol size include diameters of $0'.20$ and $0'.25$, etc. The largest circle represents all galaxies with diameters $\geq 0'.80$.

At least three pronounced structural elements are visible in Fig. 1a:

- A north-south asymmetry with respect to the number of galaxies. 71% of the galaxies are at positive b. This can be attributed to the downward bending of the galactic dust equator.
- A stripe almost free of galaxies between $(\ell, b) \approx (196°, -5°)$ and $(189°, 5°)$. Neckel & Klare (1980) found A_V values of up to $3^{\rm m}$ in that region, i.e. rather high values for anticenter fields. The distribution of dark nebulae (Lynds 1968) shows numerous dark nebulae covering this stripe.
- The most marked overdensity of galaxies appears at $(\ell, b) \approx (181.°5, +3.°5)$. Within one square degree about 40 galaxies were found there.

A comparison between Figs. 1a and b shows striking parallelism. The distribution of the $60\,\mu$ flux density seems to account for the overall distribution of the galaxies. Generally, the regions with higher $60\,\mu$ emission coincide with those of lower number density of galaxies, i.e. generally higher extinction values. For that reason we consider $A_V \propto \log(100/n)$ where n is the number of galaxies per square degree, as a practicable first approximation to guess the extinction.

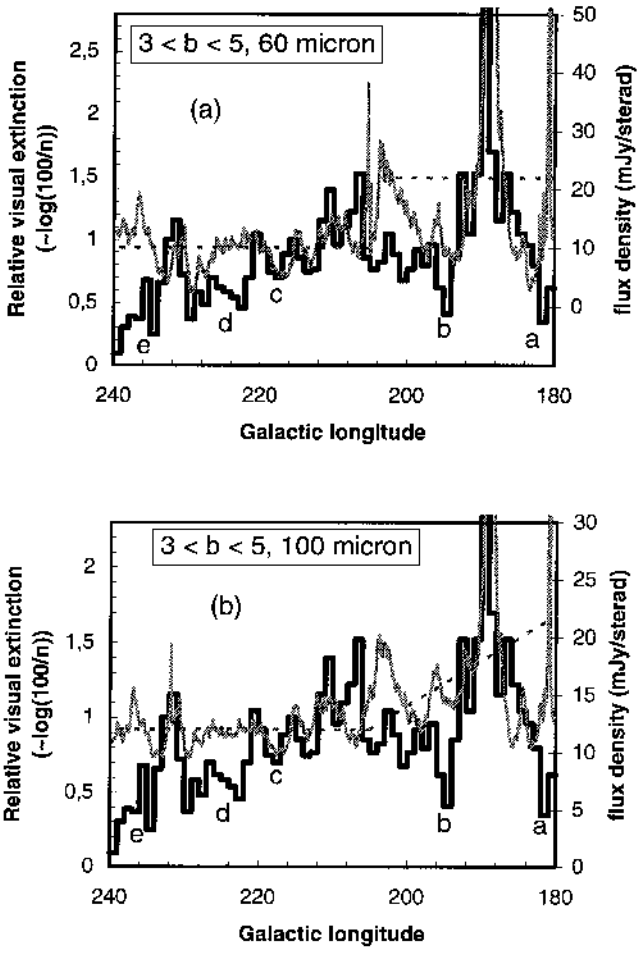

Fig. 2. Histogram of the visual extinction predicted by our galaxy counts (lefthand axis) compared with **a)** the IRAS $60\,\mu$ flux density and **b)** the IRAS $100\,\mu$ flux density (righthand axis) for the region $180° \leq \ell \leq 240°$, $3° \leq b \leq 5°$

To study the relationship between the flux densities at $60\,\mu$ and $100\,\mu$ and the galaxy counts in more detail, Fig. 2 shows a comparison of these flux densities (corrected for zodiacal emission, see below) with the extinction predicted by the number of galaxies per area for the region $180° \leq \ell \leq 240°$ and $3° \leq b \leq 5°$. The IRAS densities are represented by the grey curves (righthand axis in Fig. 2, mJy per sterad), whereas the black histogram gives predicted values for the extinction. The choice of this interval preserves statistical reliability and prevents smoothing out the data with respect to galactic latitude.

To what extent the IRAS flux densities are a measure of the total extinction within our Galaxy is under discussion nowaday. There is evidence that the $60\,\mu$ flux densities can be regarded as a good measure for the total

extinction along the line of sight (see Bloemen et al. 1990). In addition, the integrated H I emission given by Bloemen (1983) is in good agreement with the 60 μ emission. A relationship between the 100 μ and the total extinction was suggested by Boulanger & Perault (1988) and Wakamatsu et al. (1994).

However, an interpretation of IRAS flux densities faces the problems of possibly significant cirrus emission and residual zodiacal emission within the ecliptic plane.

To correct the data we made an eye-estimate of the trend of the residual zodiacal emission for $\ell \leq 205°$ (the dashed line in Fig. 2) and subtracted the influence of the ecliptic plane. For $\ell \geq 205°$ the dashed line gives the mean value for the emission.

These circumstances and the fact, that no absolute calibration can be done for both the flux densities and the galaxy counts make it difficult to normalize the two curves in Fig. 2. For the visual presentation we have chosen the displayed interval on both axes such that the two curves in Fig. 2 give a reasonable fit in the region $210° \leq \ell \leq 240°$, where the zodiacal emission seems to be negligible.

A further inconvenience in finding the best fit is that the histogram is statistically more reliable for low values of the relative visual extinction. Hence, the (local) depressions should preferably be considered when fitting the two curves. Our choice of the axes in Fig. 2 fits two (three in 60 μ) of the four local depressions and four of the four local peaks in the region $210° \leq \ell \leq 240°$.

In regions where the black curve is significantly below the grey one, we predict a lower extinction because of a surplus of galaxies compared to the amount of extinction (due to the flux density) and vice versa.

In the region $180° \leq \ell \leq 210°$ the peaks in the infrared emission (Fig. 2) are caused by clouds, reaching partly into the area with $b \geq 3°$, and smaller single sources.

We can identify two marked overdensities of galaxies in Fig. 2 located at $(\ell, b) \approx (181\overset{\circ}{.}5, +3\overset{\circ}{.}5)$ (a) and $(\ell, b) \approx (195°, +4\overset{\circ}{.}5)$ (b) which might represent hitherto unknown galaxy cluster candidates. They are indicated both by the 60 μ and the 100 μ flux densities.

3.3. *IRAS two-colour diagrams*

Out of our sample of 755 galaxies, 8.3% (63 galaxies) have IRAS counterparts, i.e. 0.21 galaxies per square degree. This value is in good agreement with the S90 survey (0.16) as well as with other surveys performed by us in the ZOA: 0.22 (Lercher & Weinberger 1995), 0.19 (Seeberger 1995). There are 52 IRAS sources with $f(60) > 0.6$ Jy, i.e. 0.17 IRAS galaxies per square degree. This is about 40% of the value published by Rowan-Robinson et al. (1990) who give 0.42 galaxies per square degree for the whole sky with $|b| \geq 10°$. Strauss et al. (1992) found 0.07 galaxies per square degree with $f(60) > 1.936$ Jy. With this flux limit we find 0.05 galaxies per square degree in our survey, i.e. 70% of the value of Strauss et al. (1992).

The two-colour distributions of these galaxies are in good agreement with published data (see, e.g., Paper I and references therein). As in Paper I, we selected only IRAS sources having a flux quality ≥ 2 for the three fluxes used in each diagram. As an example, Fig. 3 gives the IRAS two-colour diagram $\log[f(60)/f(100)]$ versus $\log[f(25)/f(60)]$, where $f(\lambda)$ is in Jy without colour correction.

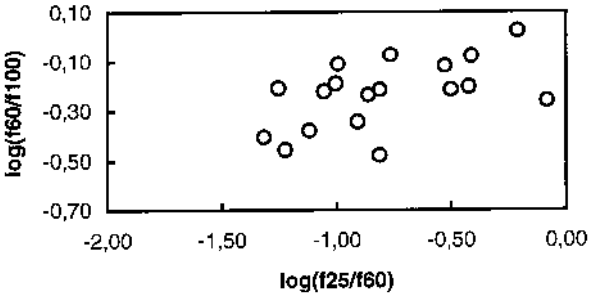

Fig. 3. IRAS two-colour diagram $\log[f(60)/f(100)]$ versus $\log[f(25)/f(60)]$ for 18 galaxies of our sample

Combining the results of Paper I and this paper we get:

$$\log f(12)/f(25) = -0.34 \pm 0.29 \qquad \text{(67 galaxies)}$$

$$\log f(25)/f(60) = -0.87 \pm 0.26 \qquad \text{(103 galaxies)}$$

$$\log f(60)/f(100) = -0.31 \pm 0.15 \qquad \text{(95 galaxies)}$$

The errors given for the flux ratios are standard deviations for each of the two samples.

4. Galaxy distribution between 210° and 240° longitude

We have extended our galaxy search to $\delta = -27°$, the declination limit of the POSS I. Therefore, about 300 square degrees have been searched for galaxies twice on a different plate material: Saitō et al. (1990) and (1991) found 1136 new galaxies in the region $210° \leq \ell \leq 240°$, $-5° \leq b \leq +5°$ (the "CGMW" catalogue) on film copies of the UK-Schmidt Southern Infrared Atlas of the Milky Way.

Figure 4a shows all galaxies found by the two independent surveys. Galaxies found by Saitō et al. (1990, 1991) are marked by squares, 334 galaxies additionally found by us are symbolized by open circles. For both symbols the size has the same meaning as in Fig. 1. Table 3 lists these additional galaxies, where the columns are the same as in Table 2. Most of them lie between $\ell = 210°$ and 220°. In subsection 5.2 we will outline that our survey is more complete in the northern part whereas the CGMW contains a significantly larger number of galaxies in the south.

Figure 4b gives the grey scale map of the IRAS 60 μ flux densities of this region.

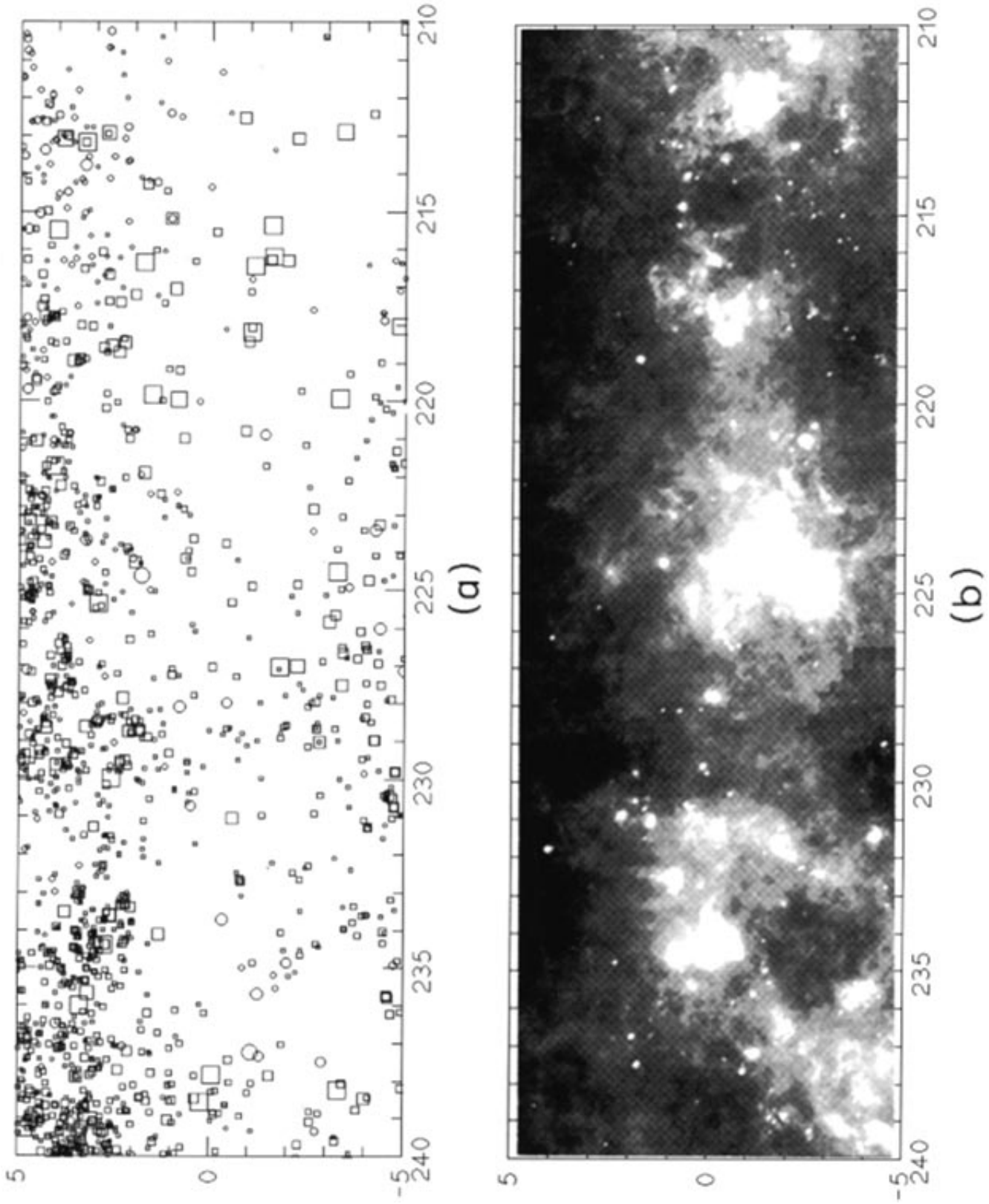

Fig. 4. a) Distribution of the newly detected additional galaxies (circles) and the CGMW-sample (squares) in galactic coordinates; **b)** the 60 μ flux density taken from the IRAS Sky Survey Atlas. Black (white) areas correspond to low (high) flux densities. **(To be seen in landscape)**

To study the distribution of galaxies in this region we again use Fig. 2. Two marked overdensities of galaxies can be found (d, e). Yamada & Saitō (1993) claimed to have found three new galaxy clusters, which are located in this region. The overdensity (d) coincides with the galaxy clusters B and C of Yamada & Saitō (1993). Their cluster A can also be seen in Fig. 2 (marked with c), but according to this figure one might expect that it is rather caused by low extinction. The concentration named (d) in Fig. 2 appears to belong to the clusters of galaxies around $\ell \approx 240°$, $b \approx +4°$ found by Saitō et al. (1991).

5. Completeness check

There is no way to obtain a magnitude-limited sample of galaxies near the galactic plane due to the patchiness of galactic extinction. The only achievable completeness refers to a certain diameter limit. Figure 5 shows the diameter distribution of the additional galaxies. Very few could be found with diameters $> 0\farcm4$. This confirms that the CGMW is almost complete for diameters $> 0\farcm4$.

A few Palomar prints have been inspected twice independently for completeness check purposes. Up to about 20% of the small diameter galaxies ($\leq 0\farcm3$) have been missed.

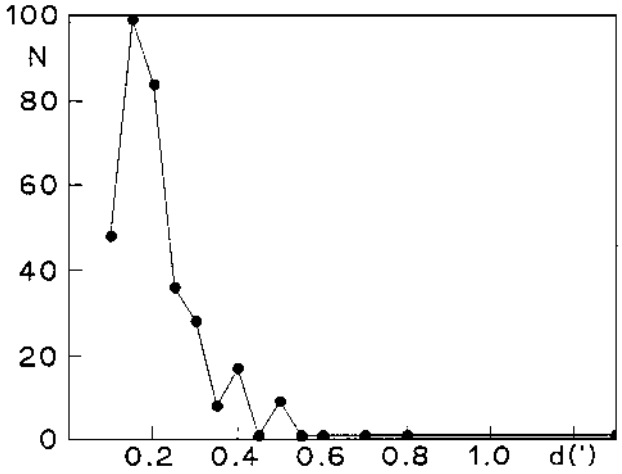

Fig. 5. Number of the galaxies additionally found in the region $210° \leq \ell \leq 240°$ as a function of their diameters

5.1. *Size distribution function*

A slope of -3 in the size distribution function indicates a complete size limited sample down to a certain diameter limit where the number of galaxies drops below the theoretical line (assumption of homogeneously distributed galaxies with a typical mean physical diameter).

Figures 6 and 7a, b show that both surveys are complete for diameters larger than $0\farcm4$. In both surveys about 50 % of the $0\farcm2$ sized galaxies could be found. Only 10%

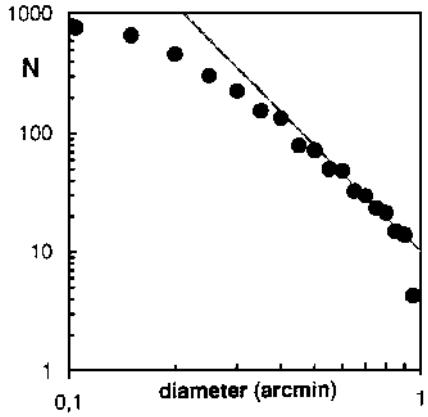

Fig. 6. Size distribution function for our survey: $180° \leq \ell \leq 210°$. N is the number of galaxies with diameters larger than the values given at the abscissa

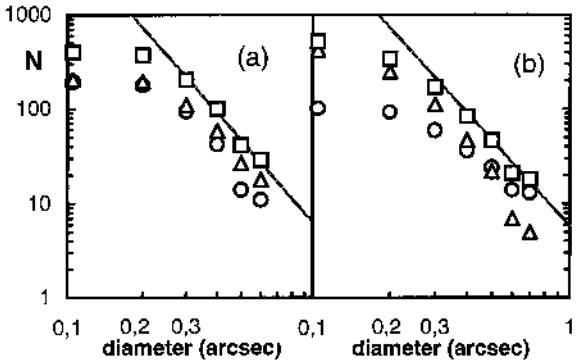

Fig. 7. Size distribution function in three longitude bins: **a)** our survey, **b)** survey of Saitō et al. (1990). Circles: $210° \leq \ell \leq 220°$, triangles: $220° \leq \ell \leq 230°$, squares: $210° \leq \ell \leq 230°$. N is the number of galaxies with diameters larger than the values given at the abscissa

of the expected number of galaxies were found with diameters of $0\farcm1$. Extinction effects cannot be responsible for the severe incompleteness at small diameters. The diameter reduction of the galaxies by extinction causes a parallel shift of the theoretical line towards smaller galaxy counts.

The diameter distribution of the galaxies in the region $180° \leq \ell \leq 210°$ is very similar to Fig. 5. The majority (91%) has diameters $\leq 0\farcm4$. The maximum number appears at a diameter of $0\farcm15$. Tiny galaxies (diameter $0\farcm1$ corresponding to 0.1 mm on the POSS) are often difficult to distinguish from stars. Therefore we rejected many of the $0\farcm1$ candidates which led to a maximum number at $0\farcm15$.

A certain fraction of the search field is covered by stellar images. This reduces the detection rate for small-diameter galaxies. To estimate the area covered by stars we used a frame grabber and digitized several small fields ($\approx 30\,\mathrm{arcmin}^2$) evenly distributed between $0° \leq b \leq 5°$.

This area (including stellar halos) amounts to 15−25%. We took into account the effect that a galaxy partly distorted by a stellar image will enlarge this area by a factor of two. Almost all missing 0′.2−diameter galaxies are explainable this way. Nevertheless, almost 50% of the 0′.1−diameter galaxies are still missing, but 0′.1 is our detectability limit for galaxies. Note that we had been very cautious in considering an object as a galaxy in order to keep the catalogue free of plate errors and other sources.

5.2. *CGMW and ZOAG catalogues*

About 200 square degrees of the ZOA ($210° \leq \ell \leq 230°$, $-5° \leq b \leq +5°$) have been surveyed twice on different plate materials by different authors: Saitō et al. (1990) on film copies of the UK Schmidt Southern Infrared Atlas (UKSSI, Hartley & Dawe 1981) and our group (this paper) on POSS I-E prints. We will compare the results.
There are 154 galaxies that were detected in both surveys. Another 249 galaxies were found on POSS I (ZOAG-survey) and 377 additional galaxies on UKSSI (CGMW-survey). The distribution is very similar in both surveys with respect to galactic latitude (see Fig. 4a). But as can be seen in Fig. 7 it differs significantly with respect to galactic longitude. Whereas the galaxy density slightly decreases with increasing longitude in the ZOAG-survey, the vast majority of the galaxies was found between $220° \leq \ell \leq 230°$ in the CGMW-survey. By considering only larger diameter galaxies (e.g. $\geqq 0'.4$, a diameter limit for which both surveys claim to be nearly complete) the general galaxy density pattern remains conserved in the ZOAG-survey, but the extreme galaxy overdensity at larger ℓ disappears in the CGMW-survey.

Measurements of the interstellar extinction in this region are at variance: Neckel & Klare (1980) found an increase in A_V from $\ell = 230°$ ($\lessapprox 1$ mag) to $\ell = 210°$ ($\gtrapprox 2$ mag). On the other hand, contour maps of H I 21-cm line intensities (Bloemen 1983; Saitō et al. 1990) show the contours to be parallel to b in the regarded longitude range.

We have searched at the position of the 377 additional galaxies found in the CGMW-survey for corresponding objects on the POSS I. About 10% could be identified as galaxies there. In the other cases neither a galaxy was found nor was a nebulous object unambiguously visible.

There is a tendency that the POSS I-plates near $\ell = 210°$ were taken under better seeing conditions compared to those at $\ell = 230°$ ($1'' - 2''$ and $3'' - 4''$, respectively; see Table 1). Another explanation why galaxies near the limit of visibility can be better recognized in the CGMW-compared to the ZOAG-survey, is the difference in airmass at which the plates were taken. For example, faint stars occupy a larger area with increasing airmass. These stars are practically indiscernible from small-diameter galaxies.

6. The best suited plate material

For the southernmost part of our survey both ESO/SERC, UK Infrared and POSS plates are available; we compared their suitability for galaxy searches and provide a recipe for future optical surveys of this type.

We surveyed the area of the southern field no. 560 centered at $\ell \approx 237°, b \approx +2°$ on POSS I-E, UK Schmidt Southern Infrared Atlas (UKSSI, Hartley & Dawe 1981), and SERC J prints or film copies. 588 galaxy candidates were detected on SERC J, 352 galaxies on UKSSI, and 94 on POSS I-E.

As to the lowest number, one should however, take into account that the POSS plate for this region was taken at an airmass of 1.7, leading to an a priori distinct decrease in image quality. The fact that the number of galaxies on the UKSSI copy is distinctly lower than that on the (blue) SERC J copy is, however, not at all obvious.

Cameron (1990) has pointed out that there is a significant reduction of the diameter at extinctions larger than about one magnitude; e.g. a spiral galaxy quickly "looses" its outer regions and the bulge is left over. This finding eases our argumentation, since bulges of spiral galaxies and elliptical galaxies have very similar and rather well defined intrinsic colours, $(B-V)_0 = +0.9 \pm 0.1$ and $(U-B)_0 = +0.45 \pm 0.15$ (de Vaucouleurs 1976). In the following, we give the major sky surveys together with their approximate effective wavelengths (Å) and limiting (stellar) magnitudes.

POSS I-O(4100, 21.1); POSS II-B(4800, 22.5); SERC J(4800, 22.5); POSS I-E(6500, 20.0); POSS II-R(6500, 20.8); ESO R(6500, 21.5); UKSSI(7900, 19.0); POSS II-IR(8500, 19.5). The red-sensitive surveys and the POSS II-IR correspond to the Cousins system.

For E and S0 galaxies the extensive VRI aperture photometry in the Cousins system was reviewed by Buta (1995), leading to $(V-R)_0 \approx +0.55$ and $(V-I)_0 \approx +1.20$ (his Fig. 3). With these data and the above given de Vaucouleurs (1976) colours, we calculated intrinsic colours $(V-X)_0$ and absolute magnitudes for the various sky survey passbands, assuming an absolute visual magnitude of $M_V = -21.7$, i.e. slightly brighter than M 31, as an object we followed through several stages of visual obscuration using the average interstellar extinction curve of Savage & Mathis (1979).

We assumed (from our practical experience) that a galaxy can easily be recognized on these Schmidt surveys if it is about 2 to 3 magnitudes below the stellar limiting magnitude. As a reference value we used a fixed apparent magnitude of $B = J = 20.0$ mag, i.e. 2.5 mag below the limiting magnitude of the POSS II-B or SERC J survey for each value of A_V, corresponding to a galaxy with $M_V = -21.7$ at 100 Mpc and $A_V = 5^{\rm m}$.

Briefly, the larger the difference between the respective (stellar) limiting magnitude of a specific survey and the apparent magnitude, the more galaxies should be

detectable, with 2.5 mag as minimum for the ability to recognize them as a galaxy.

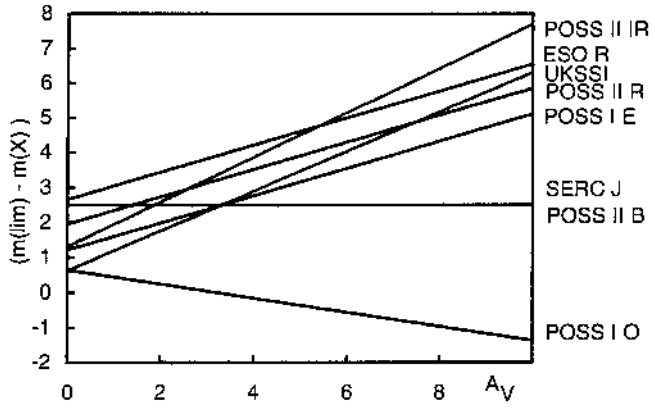

Fig. 8. Stellar limiting magnitude minus apparent magnitude for a galaxy with $M_V = -21.7$ and B=J=20 (fixed for each value of A_V) versus A_V for the various surveys. We assume that we deal with ellipticals, S0 galaxies, and the bulges of spirals

In Fig. 8 we give an overview on our results; they can be taken as a recipe for future optical surveys for galaxies except for spiral galaxies with $A_V \lessapprox 1^m - 2^m$, since at these low obscurations galaxy images retain their spiral arms. In addition it should be taken into account that galaxies obscured with $A_V \gtrapprox 6^m - 7^m$ will probably not be detectable: even the intrinsically bright nearby galaxy Maffei 2, visible on POSS I-E as an inconspicuous small smudge, suffers from $A_V \approx 6^m$, but is the most heavily obscured object in Table 2 of Paper I.

Figure 8 clearly shows that for the southern sky the use of ESO R is the best choice and is, under all circumstances, preferable to UKSSI. On the northern sky, for very small obscurations, POSS II-B might be best, but usually POSS II-R and POSS II-IR should be used instead.

The galaxy detections in field 560 on SERC J (588 candidates), UKSSI (352), and the POSS I-E prints (94) can thus be understood as follows: the comparatively small number of galaxy candidates on POSS I-E is due to the unfavourable limiting magnitude, the high air mass, and the coarse grain emulsion. The higher number of candidates on the blue J film copy compared to the IR copy, however, points to a total visual extinction of $\approx 2^m$ or less as can be deduced from Fig. 8. At these low obscurations most of the spirals retain their spiral arms and are thus easier recognizable also at very faint apparent magnitudes leading to an additional increase in the number of galaxy candidates on the J copy. A final support for our interpretation of a low obscuration in field 560 can be found in the $A_V(r)$-diagrams of Neckel & Klare (1980): their areas 86 and 87, at $(\ell, b) = (236/0)$ and $(238/0)$, respectively, although centered in the galactic plane, show only $\approx 1^m$ up to about 5 kpc distance.

Acknowledgements. This work has been supported by the "Fonds zur Förderung der wissenschaftlichen Forschung", projekt No. P8325–PHY and partly by the "Jubiläumsfonds der österreichischen Nationalbank", project No. 4713. We want to thank G. Lercher, W. Benger, Ch. Kienel, and M. Schgraffer for various support. We also thank the referee, Dr. G. Paturel, for his valuable comments.

References

Bloemen J.B.G.M., 1983, Survey of the Southern Galaxy Astrophys. Space Sci. Library, Vol. 105. In: Burton W.B. and Israel F.P. (eds.). D. Reidel Publ. Comp., Dordrecht, p. 307
Bloemen J.B.G.M., Deul E.R., Thaddeus P., 1990, A&A 233, 437
Boulanger F., Perault M., 1988, ApJ 330, 964
Burton W.B., Hartmann D., 1994, in: Balkowski C., Kraan-Korteweg R.C. (eds.) ASP Conf. Ser. 67, 31
Buta R., 1995, Astrophys. Lett. Comm. 31, 109
Cameron L.M., 1990, A&A 233, 16
de Vaucouleurs G., 1976, Le Monde des Galaxies. In: Hayli A. (ed.), Observatoire de Besancon
Dewhirst D.W., 1963, Radio Astronomy Today, Manchester. Manchester University Press
Hartley M., Dawe J.A., 1981, Proc. Astron. Soc. Aust. 4, 251
Helou G., 1986, ApJ 311, L33
Henning P.A., 1992, ApJS 78, 365
Hoessel J.G., Elias J.H., Wade R.A., Huchra J.P., 1979, PASP 91, 41
Lercher G., Weinberger R., 1995 (in preparation)
Kerr F.J., Henning P.A., 1987, ApJ 320, L99
Lu N.Y., Dow M.W., Houck J.R., Salpeter E.E., 1990, ApJ 357, 388
Lynds B.T., 1968, Stars and Stellar Systems VII, 119
Maddox S.J., Sutherland W.J., Efstathiou G., Loveday J., 1990, MNRAS 243, 692
Neckel Th., Klare G., 1980, A&AS 42, 251
Rowan-Robinson M., Lawrence A., Saunders W., et al., 1990, MNRAS 247, 1
Saitō M., Ohtani H., Asomuna A., et al., 1990, PASJ 42, 603
Saitō M., Ohtani H., Baba A., et al., 1991, PASJ 43, 449
Savage B.D., Mathis J.S., 1979, ARA&A 17, 73
Seeberger R., Huchtmeier W.K., Weinberger R., 1994, A&A 286, 17
Seeberger R., 1994, doctoral thesis, University of Innsbruck
Seeberger R., 1995, PASP 107, 1
Strauss M.A., Davis M., Yahil A., Huchra J.P., 1992, ApJ 385, 421
Takata T., Yamada T., Saitō M., Chamaraux P., Kazés I., 1994, A&AS 104, 529
Wakamatsu K., Hasegawa T., Karoji H., et al., 1994, in: Balkowski C., Kraan-Korteweg R.C. (eds.), ASP Conf. Ser., 67, 131
Weinberger R., 1980, A&AS 40, 123
Weinberger R., Saurer W., Seeberger R., 1995, A&AS 110, 269
Wheelock S., Gautier T.N., Chillemi J., et al., 1991, IRAS Sky Survey Atlas Explanatory Supplement
Yamada T., Takata T., Djamaluddin T., et al., 1993, ApJS 89, 35
Yamada T., Saitō M., 1993, PASJ 45, 25

Table 2. Optically detected galaxies in the region $180^\circ \leq \ell \leq 210^\circ, b = \pm 5^\circ$. (Only available in electronic form at the CDS)

ZOAG G	α(1950)	δ(1950)	α(2000)	δ(2000)	print	x(mm)	y(mm)	⌀ E	⌀$_c$ E	⌀ O	⌀$_c$ O	t	cross id.
180.03−2.15:	05 34 14	+27 44.7	05 37 23	+27 46.5	1459	291.0	54.7	0.25		0.15			IRAS 05342+2744
180.08+3.23	05 55 23	+30 30.5	05 58 36	+30 30.7	1459	43.9	202.3	0.25		0.20			
180.17+1.27	05 47 50	+29 25.9	05 51 01	+29 26.7	1459	130.6	143.5	0.35		0.20			IRAS 05478+2926[a]
180.19+1.03	05 46 55	+29 17.5	05 50 06	+29 18.3	1459	141.3	136.0	0.15		0.05			
180.19+3.72	05 57 37	+30 39.5	06 00 50	+30 39.6	1459	18.2	211.0	0.20		0.25	0.10		
180.20+3.66	05 57 25	+30 37.1	06 00 38	+30 37.2	1459	20.5	208.7	0.20		0.15	0.05		IRAS 05574+3037
180.22+3.46	05 56 38	+30 30.0	05 59 51	+30 30.1	1459	29.5	202.2	0.40	0.10	0.20			
180.24+0.68	05 45 41	+29 04.3	05 48 52	+29 05.2	1459	155.6	124.3	0.20	0.10				
180.27+1.36	05 48 24	+29 23.9	05 51 35	+29 24.6	1459	123.9	141.8	0.30	0.10	0.30			
180.35+1.19	05 47 54	+29 14.2	05 51 05	+29 15.0	1459	129.6	133.1	0.20		0.05			
180.35+4.54	06 01 18	+30 55.2	06 04 32	+30 55.0	411	270.2	225.1	0.40	0.15	0.10			
180.38+4.47	06 01 04	+30 51.9	06 04 18	+30 51.7	411	273.0	222.1	0.20	0.05	0.10			
180.42+3.31	05 56 31	+30 15.6	05 59 44	+30 15.7	1459	30.5	189.3	0.15		0.10			
180.48−0.96	05 39 53	+28 00.2	05 43 02	+28 01.5	1459	224.0	67.5	0.30		0.10			WEIN 149
180.50+3.09:	05 55 48	+30 04.7	05 59 00	+30 04.9	411	334.8	181.6	0.25		0.25			
180.50+3.32	05 56 43	+30 11.7	05 59 56	+30 11.8	1459	28.0	185.9	0.30		0.40			
180.51+2.82	05 54 46	+29 56.2	05 57 58	+29 56.5	1459	50.4	171.6	0.15		0.10			
180.53−3.78	05 29 18	+26 26.4	05 32 25	+26 28.5	454	34.7	298.9	0.15		0.10			
180.58+3.65	05 58 15	+30 16.8	06 01 28	+30 16.8	411	306.2	191.6	0.20	0.05	0.15			
180.59+3.51	05 57 42	+30 12.5	06 00 55	+30 12.6	411	312.6	188.0	0.15					
180.66+2.73:	05 54 45	+29 45.7	05 57 57	+29 46.0	1459	50.4	162.2	0.25		0.20			
180.70+3.29	05 57 04	+30 00.3	06 00 16	+30 00.4	411	320.2	177.2	0.60	0.20	0.20			
180.71+4.51	06 02 01	+30 35.6	06 05 14	+30 35.3	411	262.4	207.5	0.10					
180.73−2.52	05 34 34	+26 57.4	05 37 42	+26 59.1	1459	288.0	12.5	0.15		0.15			IRAS 05345+2657
180.77+3.54	05 58 15	+30 03.9	06 01 27	+30 03.9	1459	10.0	179.5	0.10		0.10			IRAS 05582+3004
180.80+3.38	05 57 40	+29 57.6	06 00 52	+29 57.7	411	313.3	174.7	0.50		0.20			
180.82+3.34	05 57 32	+29 55.3	06 00 44	+29 55.4	411	314.8	172.7	0.20		0.15			
180.83+3.99	06 00 11	+30 14.3	06 03 24	+30 14.2	411	283.9	188.9	0.50		0.50			IRAS 06001+3014
180.84+3.44	05 58 00	+29 57.4	06 01 12	+29 57.4	1459	12.9	173.6	0.20		0.15			
180.86+4.73	06 03 16	+30 34.3	06 06 29	+30 33.9	411	248.0	206.1	0.15		0.10			
180.90+3.67	05 59 03	+30 01.4	06 02 15	+30 01.4	411	297.1	177.7	0.20		0.10			
180.90+3.75:	05 59 21	+30 03.3	06 02 33	+30 03.2	411	293.6	179.3	0.20		0.10			
180.92+3.36:	05 57 50	+29 50.7	06 01 02	+29 50.7	411	311.4	168.5	0.20		0.05			
180.94+2.42	05 54 11	+29 21.5	05 57 22	+29 21.8	1459	56.5	140.5	0.25		0.20			
180.95+2.16	05 53 09	+29 13.0	05 56 20	+29 13.4	1459	68.3	132.7	0.25	0.05	0.15			
180.96+3.60	05 58 54	+29 56.0	06 02 06	+29 56.0	411	299.0	172.9	0.35		0.30		S?	
180.97+1.07	05 48 55	+28 38.4	05 52 05	+28 39.1	1459	117.5	101.3	0.10		0.15			
180.97+2.87:	05 56 02	+29 33.8	05 59 14	+29 34.0	1459	35.2	152.0	0.10		0.20			
180.98+2.88	05 56 04	+29 33.2	05 59 16	+29 33.4	1459	34.8	151.4	0.15		0.15	0.05		
181.02+3.71	05 59 29	+29 56.1	06 02 41	+29 56.0	411	292.3	172.8	0.20		0.10			
181.03+3.22	05 57 35	+29 40.8	06 00 47	+29 40.9	411	314.7	159.8	0.50	0.10	0.20			
181.09+3.29	05 57 57	+29 39.8	06 01 09	+29 39.8	411	310.4	158.8	0.30		0.15			
181.09+3.54	05 58 58	+29 47.3	06 02 10	+29 47.3	411	298.5	165.2	0.40	0.10	0.40		S?	
181.12+3.52	05 58 58	+29 45.3	06 02 10	+29 45.3	411	298.4	163.4	0.35	0.20	0.15			
181.17+0.88	05 48 38	+28 22.2	05 51 48	+28 22.9	1459	120.8	86.9	0.10		0.10			WEIN 151
181.21+3.44:	05 58 50	+29 38.3	06 02 02	+29 38.3	411	300.1	157.2	0.10		0.10			
181.22+3.49	05 59 03	+29 39.1	06 02 15	+29 39.1	411	297.5	157.9	0.30	0.15	0.10			
181.23+3.55	05 59 18	+29 40.4	06 02 30	+29 40.3	411	294.6	158.9	0.20		0.10			
181.25+4.55	06 03 25	+30 08.7	06 06 38	+30 08.3	411	246.6	183.3	0.10		0.05			
181.26+3.60	05 59 36	+29 40.5	06 02 48	+29 40.4	411	291.1	158.9	0.25		0.15			
181.26+3.64	05 59 46	+29 41.5	06 02 58	+29 41.4	411	289.2	159.8	0.15	0.05	0.10			
181.27+4.04:	06 01 23	+29 53.0	06 04 35	+29 52.8	411	270.3	169.7	0.20					
181.30+3.77	06 00 21	+29 43.1	06 03 33	+29 43.0	411	282.4	161.1	0.15		0.05			
181.31+0.94	05 49 12	+28 17.4	05 52 22	+28 18.1	1459	114.0	82.6	0.15		0.10			
181.31+2.70:	05 56 07	+29 10.8	05 59 18	+29 11.0	1459	33.6	131.5	0.15		0.10			
181.32+1.76	05 52 25	+28 41.7	05 55 35	+28 42.1	1459	76.5	104.9	0.50	0.10	0.45	0.05	S	IRAS 05524+2841[b]
181.32+3.68	06 00 01	+29 39.5	06 03 13	+29 39.4	411	286.3	158.0	0.15		0.10			
181.32+3.76	06 00 23	+29 41.9	06 03 35	+29 41.8	411	282.0	160.0	0.20		0.15			
181.34+1.12	05 49 59	+28 20.9	05 53 09	+28 21.5	1459	104.9	85.8	0.20		0.20			
181.34+3.82	06 00 41	+29 42.5	06 03 53	+29 42.3	411	278.6	160.5	0.15		0.10			

a = WEIN 148
b = WEIN 152

Table 3. Optically detected galaxies in the region $210^\circ \leq \ell \lesssim 240^\circ, b = \pm 5^\circ$: an addendum to Saitō et al.'s (1990, 1991) catalogues. (Only available in electronic form at the CDS)

ZOAG G	α(1950)	δ(1950)	α(2000)	δ(2000)	print	x(mm)	y(mm)	⌀ E	⌀$_c$ E	⌀ O	⌀$_c$ O	t	cross id.
210.25+2.65	06 53 23	+03 39.6	06 56 01	+03 35.7	929	168.2	54.7	0.30		0.20			
210.32+4.88	07 01 26	+04 37.0	07 04 05	+04 32.5	929	61.1	106.2	0.25		0.15			
210.39−2.92	06 33 49	+00 58.5	06 36 24	+00 56.0	1483	106.4	229.0	0.15	0.05	0.05			
210.40+1.34:	06 48 58	+02 55.5	06 51 35	+02 51.9	929	227.0	15.3	0.15		0.10			
210.46+4.86	07 01 38	+04 29.0	07 04 17	+04 24.5	929	58.4	99.2	0.30		0.20			
210.68+2.66:	06 54 10	+03 16.8	06 56 47	+03 12.8	929	157.6	34.4	0.15					
210.68+2.71:	06 54 22	+03 18.1	06 56 59	+03 14.1	929	155.1	35.6	0.20		0.20			
210.76+4.85:	07 02 09	+04 12.7	07 04 47	+04 08.1	929	51.3	84.7	0.30	0.10	0.40	0.10		
210.81+2.35:	06 53 20	+03 01.4	06 55 57	+02 57.5	1346	168.2	338.8	0.10					
210.82+4.76:	07 01 56	+04 07.4	07 04 34	+04 02.8	929	54.2	80.0	0.20		0.20			
211.04+1.19	06 49 36	+02 17.1	06 52 12	+02 13.4	1346	217.9	299.1	0.20		0.15			IRAS 06495+0217
211.21+4.72	07 02 30	+03 45.0	07 05 08	+03 40.4	929	46.5	60.1	0.25	0.05	0.15			
211.27+3.78	06 59 16	+03 16.3	07 01 53	+03 11.9	929	89.5	34.2	0.15		0.20			
211.33−0.24	06 45 05	+01 22.6	06 47 40	+01 19.2	1346	278.2	250.5	0.25					
211.40+2.34:	06 54 23	+02 29.6	06 57 00	+02 25.6	1346	154.2	310.5	0.15					
211.46+4.94	07 03 43	+03 38.2	07 06 21	+03 33.5	929	30.2	54.1	0.15		0.15			
211.47+4.96	07 03 49	+03 38.0	07 06 27	+03 33.3	929	28.9	53.9	0.35	0.10	0.35			
211.80+3.50	06 59 13	+02 40.3	07 01 50	+02 35.9	1346	89.5	320.2	0.20		0.10			
211.93+4.19	07 01 55	+02 52.8	07 04 32	+02 48.3	1346	53.5	331.5	0.25	0.10	0.15			
211.98+2.24	06 55 06	+01 56.3	06 57 42	+01 52.2	1346	144.5	280.9	0.15		0.10			IRAS 06551+0156
212.12+1.36:	06 52 14	+01 24.4	06 54 49	+01 20.5	1346	182.6	252.4	0.10		0.10			
212.20+4.25	07 02 38	+02 40.0	07 05 15	+02 35.4	1346	43.9	320.2	0.20	0.10	0.10			
212.38+1.09	06 51 43	+01 03.2	06 54 18	+00 59.4	1346	189.5	233.4	0.35		0.10			
212.39−0.47	06 46 12	+00 19.6	06 48 46	+00 16.2	1346	263.1	194.4	0.10					
212.43+4.00	07 02 09	+02 20.6	07 04 45	+02 16.0	1346	50.3	302.9	0.30	0.15	0.20	0.05		
212.49+0.82	06 50 58	+00 50.0	06 53 33	+00 46.2	1346	199.4	221.7	0.20					
212.51+3.65	07 01 04	+02 07.0	07 03 40	+02 02.5	1346	64.7	290.7	0.25	0.10	0.20			
212.51+4.47	07 04 00	+02 29.6	07 06 36	+02 24.9	1346	25.6	311.0	0.10		0.10			
212.58+4.15	07 02 57	+02 16.8	07 05 33	+02 12.2	1346	39.5	299.5	0.15		0.10			
212.60+4.23	07 03 18	+02 18.3	07 05 54	+02 13.7	1346	34.9	300.9	0.15		0.15			
212.60+4.61:	07 04 39	+02 28.5	07 07 15	+02 23.8	1346	16.9	310.1	0.30	0.05	0.30			
212.61+4.74	07 05 08	+02 31.4	07 07 45	+02 26.6	1346	10.4	312.6	0.10		0.05			
212.62+4.73	07 05 07	+02 30.9	07 07 44	+02 26.1	1346	10.5	312.2	0.20		0.10			
212.63+4.73:	07 05 07	+02 30.2	07 07 43	+02 25.4	1346	10.5	311.6	0.15		0.05			
212.76+3.14	06 59 43	+01 39.8	07 02 19	+01 35.4	1346	82.6	266.3	0.15		0.10			
212.76+3.31	07 00 20	+01 44.5	07 02 56	+01 40.1	1346	74.4	270.5	0.15		0.20			IRAS 07003+0144
212.77+2.22	06 56 28	+01 13.4	06 59 03	+01 09.2	1346	126.1	242.7	0.30	0.10	0.10			
212.98+3.95	07 02 59	+01 49.7	07 05 35	+01 45.1	1346	38.9	275.4	0.15	0.05	0.10			
213.02+3.89	07 02 52	+01 46.3	07 05 28	+01 41.7	1346	40.6	272.3	0.15		0.15			
213.05+3.77	07 02 28	+01 41.6	07 05 04	+01 37.0	1346	45.8	268.1	0.20		0.20			
213.06+2.28:	06 57 12	+00 59.8	06 59 47	+00 55.6	1346	116.1	230.7	0.20		0.05			
213.09+4.12	07 03 47	+01 48.8	07 06 23	+01 44.1	1346	28.2	274.6	0.20					
213.13+4.08	07 03 44	+01 45.6	07 06 20	+01 40.9	1346	28.8	271.7	0.25		0.25			
213.17+3.65	07 02 16	+01 31.5	07 04 51	+01 26.9	1346	48.5	259.1	0.15		0.15			
213.17+4.22	07 04 19	+01 47.3	07 06 55	+01 42.6	1346	21.1	273.3	0.10		0.10			
213.18+3.60:	07 02 07	+01 29.5	07 04 42	+01 24.9	1346	50.4	257.4	0.10		0.10			
213.37−1.61:	06 43 58	−01 04.3	06 46 30	−01 07.6	1346	292.7	119.7	0.10					
213.38+4.40	07 05 21	+01 41.3	07 07 57	+01 36.5	1491	325.7	270.1	0.40	0.20	0.40	0.25		IRAS 07053+0141
213.53+4.91	07 07 26	+01 47.5	07 10 02	+01 42.6	1491	297.8	275.6	0.30		0.40	0.05	S?	
213.54+2.57	06 59 07	+00 42.1	07 01 41	+00 37.7	1346	90.5	214.9	0.20		0.10			
213.54+3.24	07 01 29	+01 00.6	07 04 04	+00 56.1	1346	58.9	231.6	0.25		0.20			
213.64+2.15	06 57 49	+00 25.4	07 00 23	+00 21.1	1346	107.9	200.0	0.20		0.20			
213.68+2.20	06 58 04	+00 24.4	07 00 38	+00 20.1	1346	104.4	199.2	0.20		0.05			
213.76+4.26	07 05 32	+01 17.4	07 08 07	+01 12.6	1491	323.2	248.9	0.20		0.15			
213.78+3.30	07 02 10	+00 49.8	07 04 45	+00 45.2	1346	49.6	222.0	0.50	0.10	0.50	0.10		
213.82+3.02:	07 01 14	+00 39.7	07 03 48	+00 35.2	1346	62.1	212.9	0.10		0.10			
213.85+4.59	07 06 53	+01 21.6	07 09 28	+01 16.7	1491	305.0	252.6	0.15		0.15			
214.03+4.95:	07 08 28	+01 21.6	07 11 03	+01 16.6	1491	283.9	252.6	0.15		0.15			
214.05+4.45	07 06 44	+01 06.8	07 09 19	+01 01.9	1491	307.1	239.4	0.10		0.10			
214.10+1.87	06 57 39	−00 06.8	07 00 13	−00 11.0	1346	109.9	171.4	0.15		0.15			IRAS 06576−0006